Available online at www.sciencedirect.com
SCIENCE DIRECT®
Bioorganic & Medicinal Chemistry Letters
ELSEVIER
Bioorganic & Medicinal Chemistry Letters 14 (2004) 2025–2030

The design, preparation and SAR of novel small molecule sodium (Na^+) channel blockers

Mark A. Ashwell,* Jean-Marc Lapierre, Alan Kaplan, Jenny Li, Christopher Marr and Jin Yuan

ArQule Inc., 19 Presidential Way, Woburn, MA 01801, USA

Received 28 January 2004; revised 13 February 2004; accepted 13 February 2004

Abstract—A parallel strategy incorporating predictive modeling of both sodium site 2 blocking activity and cytochrome P450 CYP2D6 enzyme activity as well as experimental data from ADME profiling (eADME) has been applied to the design of new small molecule sodium channel blockers. New structural motifs were identified, which combined sodium channel activity with decreased ADME liabilities. Compounds **10h** (site 2, IC_{50}=531 nM) and **7j** (site 2, IC_{50}=149 nM) were identified from two structural classes as sodium channel blockers with favorable in vitro eADME profiles.

As a result of in vitro biological data generated while profiling a targeted library of small molecules synthesized for their ability to affect a range of voltage-gated ion channels[1] we identified a number of sodium channel blockers. The in vitro screening showed them to be submicromolar inhibitors of the binding of [^{3}H]batrachotoxin to the neurotoxin site 2 of the sodium (Na^+) channel[2] (e.g., **1**, Fig. 1).

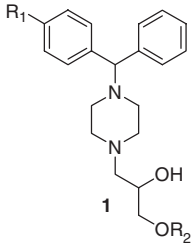

Compd	R_1	R_2	Na site 2 IC_{50} (nM)	*In silico* CYP 2D6 Ki (μM)	CYP 2D6 (% inhib. @ 2μM)	Peak TTX_r (% inhib @ 10 μM)	Peak TTX_s (% inhib @ 10 μM)
1a	CF_3	Ph	893	0.6	87	61	57
1b	Cl	allyl	401	0.1	87	20	NT

Figure 1. Predicted and measured properties of initial hits.

Currently there is considerable interest in sodium channels as therapeutically relevant biological targets with potential clinical utility[3] so compounds from these libraries were profiled further. Compounds **1a** and **1b** were therefore selected as representative compounds and functional electrophysiology studies in whole-cell patch-clamp experiments conducted in cultured rat dorsal root ganglion (DRG).[4] Compound **1a** was identified as a potent nonselective blocker of both tetrodotoxin TTX-resistant and TTX-sensitive current. **1b** was found to be considerably weaker (Fig. 1).

However, further profiling of analogs with general structure **1** across a range of in vitro ADME assays revealed an unwanted inhibitory class effect against the cytochrome P450 2D6 (CYP2D6). CYP2D6 is a minor component (approx. 2%) of total cytochrome P450 content in human liver, yet is responsible for the metabolism of a significant proportion (approx. 20%) of drugs currently in clinical use.[5] An additional complication with CYP2D6-mediated metabolism is due to genetic polymorphism in humans.[6]

We therefore considered CYP2D6 inhibition to be an undesirable property for these potentially useful, sodium channel blockers, and thus initiated a hit expansion project to increase the structural diversity beyond that of the original scaffold of **1**. We sought to identify new molecules, which maintained or improved in vitro sodium blocking activity for site 2 and were less inhibitory to CYP2D6.

* Corresponding author. Tel.: +1-781-9940598; fax: +1-781-9940690; e-mail: mashwell@arqule.com

0960-894X/$ - see front matter © 2004 Elsevier Ltd. All rights reserved.
doi:10.1016/j.bmcl.2004.02.078

A virtual library design protocol was developed incorporating in silico pharmacophore and predictive ADME screening. New designs were pre-screened in silico for their ability to fit an in-house sodium channel blocker pharmacophore model developed for site 2 binding and for their inhibition of CYP2D6.[7] Virtual library designs were thus conceived, screened in silico to assist our scaffold prioritization as well as to guide reagent selection, prior to preparation in a parallel chemistry paradigm.

Since the early SAR indicated that the R_2 substituent of **1** played a minor role in affecting CYP2D6 inhibition we focused on the removal of the benzhydryl chiral center of **1a**. Moving one of the piperazinyl nitrogens out of the ring and subsequent amide functionalization provided intermediates **3**. Compounds based on this scaffold were readily accessible,[8] as shown in Scheme 1.

tert-Butyl-4-anilinotetrahydro-1(2*H*)-pyridine carboxylates (commercially available or prepared in one-step from *tert*-butyl 4-oxo-1-piperidinecarboxylate)[9] were coupled with a variety of acid chlorides, providing intermediates **3**. Removal of the Boc group and reaction of the resulting amine with commercial 2-(aryloxymethyl)oxiranes gave **4**.

Compounds **7** were prepared according to Scheme 2. Commercially available 2-[4-[(*tert*-butyl)oxycarbonyl] piperazinyl]-2-phenylacetic acids, **5**, were reacted with amines (HBTU coupling)[10] to provide intermediates **6**. The Boc protecting group was removed and the free amine reacted with 2-(aryloxymethyl)oxiranes as shown to provide compounds of general structure **7**.

Further library synthesis is shown in Scheme 3. Commercially available 2-[4-[(*tert*-butyl)oxycarbonyl]piperazinyl]-2-phenylethylamines, **8**, were coupled with a variety of acid chlorides to give **9**. Boc deprotection and epoxide opening gave **10**. In a similar manner, intermediates **11** were obtained from the reaction of **8** with sulfonyl chlorides. Deprotection and epoxide opening provided **12**.

Our screening approach determined the in vitro sodium site 2 activity using a ligand-displacement assay measuring the ability of the compound to inhibit the binding of [^{3}H]batrachotoxin to rat cerebral cortex membranes. Single point screening at a fixed concentration was followed by IC_{50} determination for active compounds. A suite of ADME assays allowed us to assess additional in vitro parameters such as solubility, CYP inhibition, metabolic stability, etc.

Initially we sought to determine the role of the diphenylmethyl piperazine core of **1a** in determining site 2 binding as well as its influence on CYP2D6 inhibition. Significantly, the first array (**4**, Table 1) demonstrated that replacement of one of the aromatic rings with an amide group provided molecules with site 2 blocking activity. Additionally, some compounds in this array were somewhat more active (about 2- to 4-fold) than **1a** at blocking sodium site 2 (e.g., **4b** and **4e**).

From an analysis of the predicted in silico CYP2D6 inhibitions we did not expect a significant reduction in inhibition from members of this array and as shown in Table 1 the measured in vitro single point inhibition values at the screening concentration of 2 μM

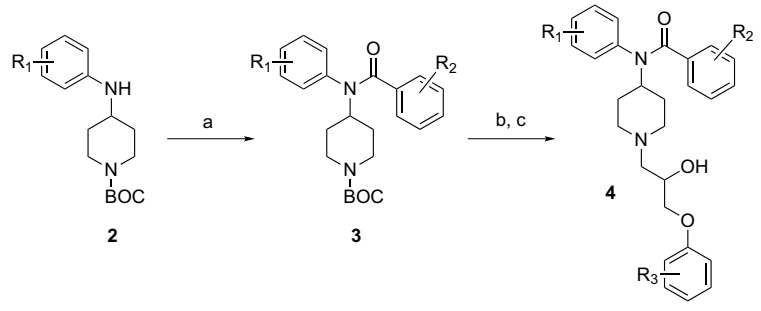

Scheme 1. Reagents and conditions: (a) ArCOCl, Hunig's base, CH_2Cl_2; (b) 4 M HCl in dioxane; (c) 2-(aryloxymethyl)oxirane, MeOH, 65 °C.

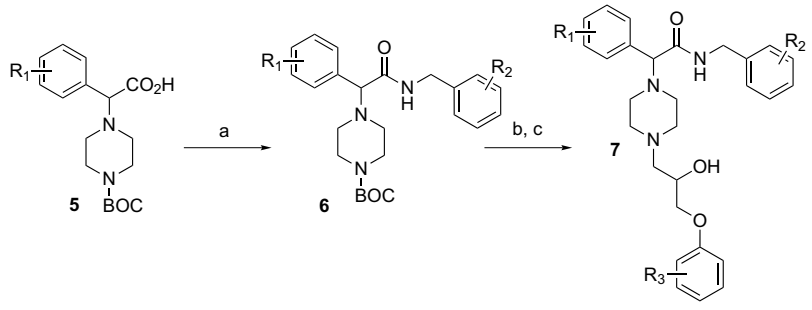

Scheme 2. Reagents and conditions: (a) amine, HBTU, Hunig's base, DMF; (b) 4 M HCl in dioxane; (c) 2-(aryloxymethyl)oxirane, MeOH, 65 °C.

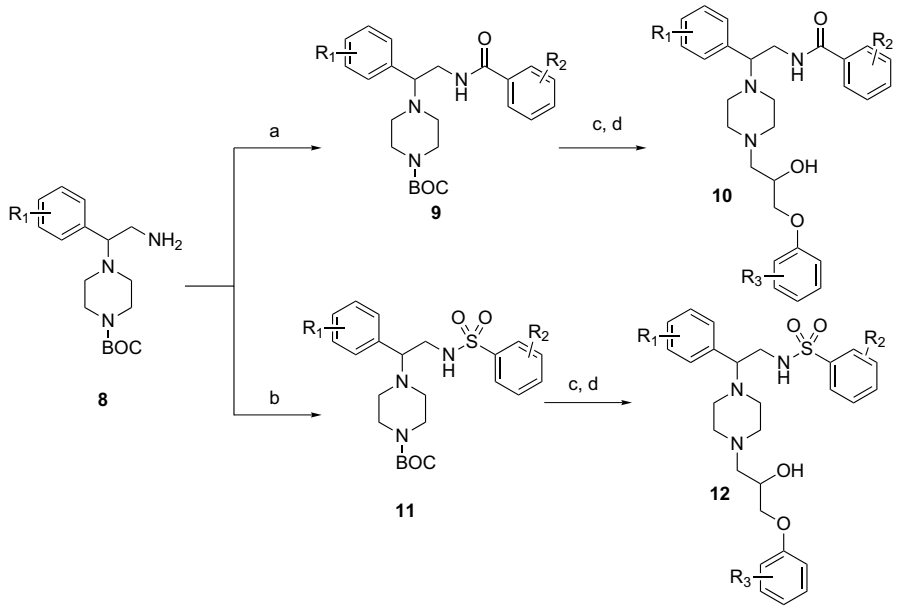

Scheme 3. Reagents and conditions: (a) acid chloride, Hunig's base, CH_2Cl_2; (b) sulfonyl chloride, pyridine, 60 °C; (c) 4 M HCl in dioxane; (d) 2-(aryloxymethyl)oxirane, MeOH, 65 °C.

Table 1. SAR of functionalized *N*-phenyl-*N*-(piperidin-4-yl)benzamides

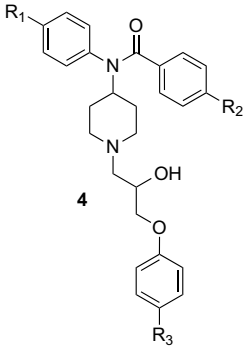

Compound	R_1	R_2	R_3	Na site 2 IC_{50} (nM)	In silico CYP 2D6 K_i (μM)	CYP 2D6 inhibition (% inhibition @ 2 μM)	HLM stability (% remaining @ $t = 30$ min)	CYP 3A4 (% inhibition @ 2 μM)
4a	H	H	OMe	261	2	34	24	71
4b	H	OMe	OMe	183	0.7	73	33	87
4c	H	Cl	OMe	228	1	71	28	90
4d	F	H	OMe	194	1	55	41	79
4e	F	OMe	OMe	191	3	68	34	88
4f	F	Cl	OMe	214	2	77	38	97

follow a similar trend to the predicted K_i values. Important SAR trends were indicated, such as a tendency for lower CYP2D6 inhibition when R_2=H (**4a** and **4d**).

Having made the important discovery that the diphenylmethyl piperazine scaffold was not a pre-requisite for site 2 activity we pursued virtual designs based on the N-alkylated *N*-phenylpiperidin-4-amine core of **2**. However, since many of the compounds in Table 1 were additionally also potent CYP3A4 inhibitors and had low stability in the isolated human liver microsome assay (HLM) we sought to identify additional alternative scaffolds without these liabilities.

One such design, **7**, in which an amide group has been introduced to replace one of the phenyl rings of the diphenylmethyl core of **1**, was expected to have reduced CYP2D6 inhibition based on our predictive model. In addition a good pharmacophore fit encouraged us to synthesize several building blocks **6** and to use these to furnish a library of compounds **7**. The sodium site 2 binding assay showed that many examples of **7** had good blocking profiles (Table 2). The most potent

Table 2. SAR of *N*-benzyl-2-phenyl-2-(piperazin-1-yl)acetamides

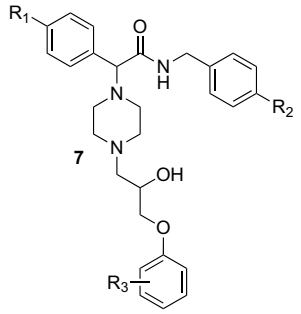

Compound	R_1	R_2	R_3	Na site 2 IC_{50} (nM)	In silico CYP 2D6 K_i (μM)	CYP 2D6 (% inhibition @ 2 μM)	HLM stability (% remaining @ $t = 30$ min)	CYP 3A4 (% inhibition @ 2 μM)
7a	Me	H	2,6-Di-Me	325	2	26	41	44
7b	Me	H	4-OMe	579	4	10	10	65
7c	Me	OMe	2,6-Di-Me	351	3	14	60	74
7d	CF_3	H	2,6-Di-Me	296	1	24	62	53
7e	CF_3	H	4-OMe	429	2	13	28	68
7f	CF_3	OMe	2,6-Di-Me	355	2	8	60	62
7g	CF_3	OMe	4-OMe	359	4	0	43	88
7h	OMe	OMe	2,6-Di-Me	571	5	9	64	74
7i	F	H	4-OMe	254	5	0	8	49
7j	F	H	2,6-Di-Me	149	2	20	57	38
7k	F	OMe	2,6-Di-Me	343	3	11	52	70
7l	F	OMe	4-OMe	214	7	10	10	81

compounds in this series were those that had electron-withdrawing groups at R_1 especially fluorine (**7i–l**).

The predicted in silico CYP2D6 inhibition values for **7** showed a trend towards reduced inhibition across the series compared to **1**. Experimentally CYP2D6 single point percentage inhibitions were below 25% in agreement with our expectations. Indeed many examples in this array were potent site 2 sodium channel blockers (below 500 nM) with little inhibition of CYP2D6 (below 25%).

However, in general, members of this series were also CYP3A4 inhibitors with low to medium HLM stability

Table 3. SAR of *N*-(2-phenyl-2-(piperazin-1-yl)ethyl)benzamides

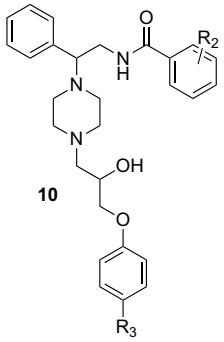

Compound	R_2	R_3	Na site 2 IC_{50} (nM)	In silico CYP 2D6 K_i (μM)	CYP 2D6 (% inhibition @ 2 μM)	HLM stability (% remaining @ $t = 30$ min)	CYP 3A4 (% inhibition @ 2 μM)
10a	H	OMe	745	4	22	8	79
10b	4-OMe	OMe	871	8	12	23	95
10c	4-OMe	Cl	538	4	47	74	96
10d	4-CF_3	OMe	253	3	12	20	94
10e	4-CF_3	Cl	208	1	40	78	69
10f	2-OMe	OMe	721	8	9	9	93
10g	2-OMe	Cl	363	7	9	39	61
10h	4-F	H	531	3	33	62	22
10i	4-F	OMe	880	5	15	6	90

Table 4. SAR of *N*-(2-phenyl-2-(piperazin-1-yl)ethyl)phenylsulfonamides

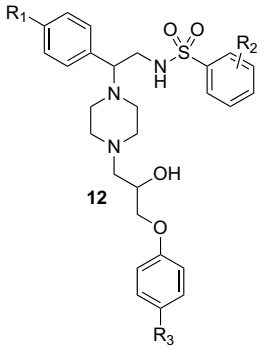

Compound	R_1	R_2	R_3	Na site 2 IC_{50} (nM)	In silico CYP 2D6 K_i (μM)	CYP 2D6 (% inhibition @ 2 μM)	HLM stability (% remaining @ $t = 30$ min)	3A4 inhibition (%)
12a	CF_3	3-Me	Br	95[a]	10	27	53	76
12b	H	2,5-Di-OMe	Br	522	30	25	77	100
12c	CF_3	2-Cl	F	76[a]	10	56	48	92

[a] % Inhibition at 1 μM.

although SAR trends showed that the introduction of methoxy groups at R_2 or R_3 was detrimental to the overall profile (e.g., compare **7l** to **7k** and **7c** to **7a**) suggesting strategies to follow beyond lead expansion.

The most potent compound in this set, **7j** was a potent site 2 binder (IC_{50}=149 nM) with no CYP2D6 inhibition, good HLM stability, and low CYP3A4 inhibition.

In another of our templates we reversed the amide of **7**, providing structure **10**. The predicted CYP2D6 values indicated that this would result in a series with a decrease in CYP2D6 inhibition. This proved to be the case when these compounds were synthesized and screened in vitro. Individual compounds were identified, which combined good blocking activity at site 2 with low CYP2D6 inhibition (e.g., **10e** and **10d** in Table 3). Again, as with scaffold **7**, additional eADME screening revealed important SAR trends such as the detrimental effect of a 4-OMe group as R_3, which resulted in reduced HLM stability and increased CYP3A4 inhibition (compare **10i** and **10h**).

It was expected from the in silico CYP2D6 model that extending the design to the sulfonamides **12** would also provide lower levels of CYP2D6 inhibition. This proved to be the case. Site 2 blockers where prepared which had reduced inhibition of CYP2D6 (**12a** and **12b**). However, **12a** and **12b** were found to be significant CYP3A4 inhibitors and so these were not pursued further (Table 4).

In conclusion we have utilized a strategy incorporating parallel in silico modeling of sodium site 2 blocking activity and CYP2D6 inhibition to identify new scaffolds. Using this approach together with in vitro biological screening we have identified a number of series of potent sodium channel blockers with a range of ADME profiles. Two series (**7** and **10**) were of particular interest for their overall favorable activity and ADME profiles. From these series **7j** and **10h** represent new structural motifs, which together with their associated SAR may provide sodium channel site 2 blockers of therapeutic value.

Acknowledgements

We thank Dr. Toan Nguyen for his molecule modeling assistance and Dr. Steve Gallion for his project leadership. In addition we also wish to acknowledge the many valuable contributions made to the voltage-gated ion channel project at ArQule, without which work described in this paper would not have been possible.

References and notes

1. (a) Gallion, S.; Hardy, L.; Sheldon, A. *Curr. Drug Discov.* **2002**, *1*, 25–27; (b) Sections of this work have been presented; http://www.chimolecularmed.com/postconpdf/mmmtrack3/mark_ashwell.pdf
2. Brown, G. B. *J. Neurosci.* **1986**, *6*, 2064–2070.
3. Anger, D.; Madge, D. J.; Mulla, M.; Riddal, D. *J. Med. Chem.* **2001**, *44*, 115–137.
4. Compounds were screened against the TTXr current recorded from dissociated rat DRG cells. Each compound was screened at a concentration of 10 μM and applied to each cell for 4 min. In addition compounds were screened against the TTXs sodium current. For more details see Elliott, A. A.; Elliott, J. R. *J. Physiol.* **1993**, *463*, 39–56.
5. Tredger, J. M.; Stoll, S. *Hosp. Pharmacist* **2002**, *9*, 167–173.
6. Bertilsson, L. *Clin. Pharmacokinet.* **1995**, *29*, 192–209.
7. The predictive competitive inhibition model for CYP2D6 was constructed from data using probe substrates and an in house compound set. The output for this model is given as a binding constant or K_i (expressed in μM). The technical details of these models will be published elsewhere.

8. All final compounds were prepared in a parallel chemistry fashion, purified by RP-HPLC and characterized by HPLC–MS, yields ranged from 10–80% based on recovered mass. In those cases were stereoisomers were generated no attempt was made to separate individual components.
9. (a) Apodaca, R.; Xiao, W. *Org. Lett.* **2001**, *3*, 1745–1748; (b) Mattson, R.; Pham, K. M.; Leuck, D. J.; Cowen, K. A. *J. Org. Chem.* **1990**, *55*, 2552–2554.
10. Knorr, R.; Trzeciak, A.; Bannwarth, W.; Gillessen, D. *Tetrahedron Lett.* **1989**, *30*, 1927–1930.